IEICE TRANSACTIONS

on Communications

VOL. E106-B NO. 2
FEBRUARY 2023

A PUBLICATION OF THE COMMUNICATIONS SOCIETY

The Institute of Electronics, Information and Communication Engineers
Kikai-Shinko-Kaikan Bldg., 5-8, Shibakoen 3chome, Minato-ku, TOKYO, 105-0011 JAPAN

PAPER

Multi-Input Physical Layer Network Coding in Two-Dimensional Wireless Multihop Networks

Hideaki TSUGITA[†], ***Nonmember***, **Satoshi DENNO**[†a)], ***and*** **Yafei HOU**[†], ***Senior Members***

SUMMARY This paper proposes multi-input physical layer network coding (multi-input PLNC) for high speed wireless communication in two-dimensional wireless multihop networks. In the proposed PLNC, all the terminals send their packets simultaneously for the neighboring relays to maximize the network throughput in the first slot, and all the relays also do the same to the neighboring terminals in the second slot. Those simultaneous signal transmissions cause multiple signals to be received at the relays and the terminals. Signal reception in the multi-input PLNC uses multichannel filtering to mitigate the difficulties caused by the multiple signal reception, which enables the two-input PLNC to be applied. In addition, a non-linear precoding is proposed to reduce the computational complexity of the signal detection at the relays and the terminals. The proposed multi-input PLNC makes all the terminals exchange their packets with the neighboring terminals in only two time slots. The performance of the proposed multi-input PLNC is confirmed by computer simulation. The proposed multi-input physical layer network coding achieves much higher network throughput than conventional techniques in a two-dimensional multihop wireless network with 7 terminals. The proposed multi-input physical layer network coding attains superior transmission performance in wireless hexagonal multihop networks, as long as more than 6 antennas are placed on the terminals and the relays.
key words: *physical layer network coding, precoding, multihop network, singular value decomposition*

1. Introduction

The provision of high quality services via smart phones and other devices such as tablets has demanded high speed wireless communications. Broadband wireless local area networks (WLANs) such as the IEEE802.11ax and the fifth generation cellular system have been launched to comply with the request. Higher frequency bands such as millimeter wave bands have been considered for such high speed wireless communication systems. For example, 60GHz band and 28GHz band are used for the IEEE802.11ad and the fifth generation cellular system in Japan. Higher frequency bands than those bands such as terahertz bands are considered for the next generation cellular system, so called, 6G. As is well known, radio signals are more attenuated in wireless channels as the carrier frequency is raised. The use of high frequency bands shortens communication distance of wireless communications, which increases service outage probability through the wireless communications in its service area. Wireless multihop communication has been considered to alleviate the outage probability problem not only in millimeter wave bands but also in microwave and UHF bands. While wireless multihop communication solves the outage problem, wireless multihop communication reduces transmission efficiency, i.e., frequency utilization efficiency. Physical layer network coding (PLNC) is known to improve the frequency utilization efficiency [1]–[7]. Because some packets collide at the nodes in multihop networks with the PLNC, sophisticated signal detection is necessary at the nodes such as the maximum likelihood detection (MLD). Since the MLD is too complex to implement at nodes, complexity reduction techniques for the PLNC have been proposed. A low complexity PLNC system has been proposed that a signal detector at a relay comprises only slicers with assistance of the precoder on the transmitter, which achieves the optimum transmission performance in spite of the low computational complexity [8]–[12]. On the other hand, the systems have been extended for multihop wireless networks in order to achieve higher frequency utilization efficiency [13]–[18]. However, the physical layer network coding has only been applied to one-dimensional multihop networks where only two terminals can send their packets.

In this paper, we propose multi-input physical layer network coding (multi-input PLNC) for high speed wireless communication in two-dimensional multihop networks. In the proposed PLNC, all the terminals send their packets simultaneously for the neighboring relays in the first slot, and after applying rateless coding such as XOR-coding to the received signals, all the relays send the packets with the coded signals to the neighboring terminals, which makes it possible to exchange all the packets with the neighboring terminals in two time slots in two-dimensional wireless multihop networks. To implement the proposed physical layer network coding, multichannel filtering is applied at the signal reception in the proposed network coding which enables two-input rateless codes to be used. In addition, we propose a non-linear precoding for the multi-input PLNC with the multichannel filtering, which reduces the signal detection complexity. The performance of the proposed PLNC is evaluated that the PLNC achieves superior performance in a hexagonal multihop network as long as more than 6 antennas are placed on the relays and the terminals.

Next section introduces a system model of a two-dimensional multihop wireless network. Section 3 explains our proposed multi-input PLNC, and the performance of the proposed PLNC is verified by simulation in Sect. 4. Finally, conclusions are remarked in Sect. 5.

Manuscript received April 8, 2022.
Manuscript revised June 30, 2022.
Manuscript publicized August 10, 2022.
[†]The authors are with Graduate School of Natural Science and Technology, Okayama University, Okayama-shi, 700-8530 Japan.
a) E-mail: denno@okayama-u.ac.jp
DOI: 10.1587/transcom.2022EBP3062

2. Two-Dimensional Multihop Network

We assume a two-dimensional multihop network in which terminals and relays are located adjacent to each other. Figure 1 illustrates a two-dimensional multihop network where relays and terminals are placed on the vertices in the network[†]. The black circles and the white circles represent terminals and relays, respectively. The packets transmitted from the vertices are assumed to only arrive at those neighboring vertices[††]. For example, the packets sent from the terminal C reach to only the relays R_2, R_3, and R_4 and those from the relay R_2 are received only at the terminals B, E, and C in the two-dimensional wireless network shown in Fig. 1. All the terminals exchange their signals with their neighboring terminals. For the signal exchange, half duplex, so called the time division duplex (TDD) is applied in the network. $N_{\rm T}$ antennas and $N_{\rm R}$ antennas are placed on the terminal and the relay, respectively. Let $\dot{Y}_2 \in \mathbb{C}^{N_{\rm R}}$ denote a received signal vector at the relay R_2, for example, the received signal vector is written as,

$$\dot{Y}_2 = \dot{H}_{2\rm B}X_{\rm B} + \dot{H}_{2\rm C}X_{\rm C} + \dot{H}_{2\rm E}X_{\rm E} + \dot{N}_2 \quad (1)$$

$\dot{H}_{2\rm B} \in \mathbb{C}^{N_{\rm R}\times N_{\rm T}}, \dot{H}_{2\rm C} \in \mathbb{C}^{N_{\rm R}\times N_{\rm T}}$, and $\dot{H}_{2\rm E} \in \mathbb{C}^{N_{\rm R}\times N_{\rm T}}$ represent channel matrices between the terminals B, C, and E and the relay R_2, respectively. $X_{\rm B} \in \mathbb{C}^{N_{\rm T}}, X_{\rm C} \in \mathbb{C}^{N_{\rm T}}$, $X_{\rm E} \in \mathbb{C}^{N_{\rm T}}$, and $\dot{N}_2 \in \mathbb{C}^{N_{\rm R}}$ denote transmission signal vectors from the terminals B, C, and E, and an additive white Gaussian noise (AWGN) vector. As is shown in (1), the three vectors are received at the relay R_2, which is regarded as packet collision. Conventionally, the collision prevents the relay from detecting the packets sent by the three neighbors. To avoid the harmful packet collision, access control techniques are used that allow only one neighbor to send the packets. When the conventional technique is used to the two-dimensional network shown in Fig. 1, the terminals have to wait for several time slots to send their own packets to their neighboring terminals. While the terminal C has 6 neighboring terminals, the other terminals have 4 neighboring terminals. Because the terminal needs 2 time slots to send their packets to their neighboring terminal, $(2 \times 4) \times 6 + 2 \times 6 = 60$ time slots are needed for all the terminals to exchange their packets with the neighbors in total[†††]. In the next section, we propose a new technique that allows all terminals to exchange packets during two time slots in the two-dimensional multihop wireless network.

[†]Such multihop networks have been utilized for the wireless smart utility network (WiSUN) and WLAN mesh networks, to which our proposed multi-input PLNC can be potentially applied. However, implementation of our proposed technique into those systems is one of our future works, because not only the hexagonal 2-D network but also other 2-D networks are formed in those networks.

[††]The assumption is justified in the section of the performance evaluation.

[†††]We can think of the communication without relaying where the terminals try to receive the packets sent by the neighboring terminals. However, the transmission performance is deteriorated due to severe signal attenuation in the channels. This is the reason why researchers and communication systems need to introduce relaying in wireless networks. Therefore, the communication without relaying is not worth considering in this paper.

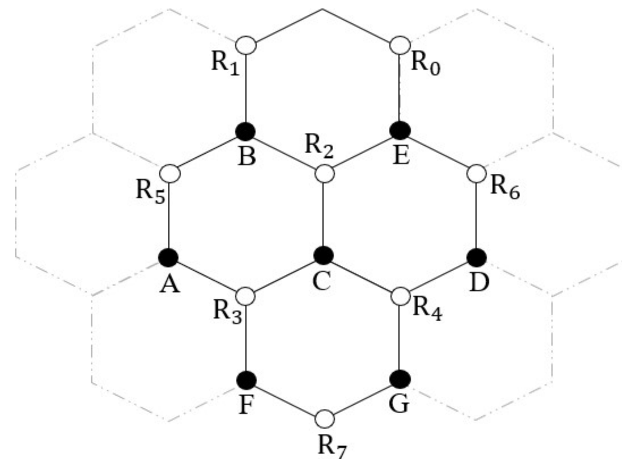

Fig. 1 Two-dimensional multihop network.

3. Multi-Input Physical Layer Network Coding

As is introduced in the previous section, all the terminals transmit their signals simultaneously. Let $N_{\rm S} \in \mathbb{N}$ and $d_\Omega \in \mathbb{C}^{N_{\rm S}}$ denote the number of the streams sent from the terminal to the neighboring terminal and a transmission signal vector sent from a terminal Ω where Ω takes one of A~G, the vectors $d_{\rm B}$, $d_{\rm C}$, and $d_{\rm E}$ are received at the relay R_2, for example. The proposed technique applies a rateless code such as an XOR-coding to those received signal vectors, e.g., $d_{2\rm BC} = d_{\rm C} \oplus d_{\rm B} \in \mathbb{C}^{N_{\rm S}}$, $d_{2\rm CE} = d_{\rm C} \oplus d_{\rm E} \in \mathbb{C}^{N_{\rm S}}$, and $d_{2\rm BE} = d_{\rm B} \oplus d_{\rm E} \in \mathbb{C}^{N_{\rm S}}$ where $\oplus$ indicates the XOR-coding.

In the second slot, the relay R_n transmits the encoded signal vectors $d_{n\Omega_1\Omega_2}$ and $d_{n\Omega_1\Omega_3}$ to the terminal Ω_1 where the terminals $\Omega_m, m = 1 \sim 3$ are the three neighbors to the relay R_n. In other words, all the relays send the encoded signal vectors so as to deliver $N_{\rm S}$ signals to their neighboring terminals. The terminals receive all the signal vectors sent from the neighboring three relays. For example, the terminal C receives the signals $d_{2\rm CB}$, $d_{2\rm CE}$, $d_{3\rm CA}$, $d_{3\rm CF}$, $d_{4\rm CD}$, and $d_{4\rm CG}$. The terminals detect all the signals delivered by the three neighboring relays. Given the $6N_{\rm S}$ detected signals, the terminal can obtain all the transmission signal vectors sent by all the neighboring terminals. For example, if the signal vectors $d_{2\rm CB}$, $d_{2\rm CE}$, $d_{3\rm CA}$, $d_{3\rm CF}$, $d_{4\rm CD}$, and $d_{4\rm CG}$ are detected at the terminal C, all the signal vectors can be obtained with the XOR operation as,

$$\begin{aligned}
&[d_{2\rm CB}\ d_{2\rm CE}\ d_{3\rm CA}\ d_{3\rm CF}\ d_{4\rm CD}\ d_{4\rm CG}] \oplus d_{\rm C} \\
&= [d_{\rm C} \oplus d_{\rm E} \oplus d_{\rm C}\ \ d_{\rm C} \oplus d_{\rm B} \oplus d_{\rm C}\ \ d_{\rm C} \oplus d_{\rm A} \oplus d_{\rm C}, \cdots] \\
&= [d_{\rm E}\ d_{\rm B}\ d_{\rm A}\ d_{\rm F}\ d_{\rm D}\ d_{\rm G}]\,. \quad (2)
\end{aligned}$$

The terminal C gets all the signal vectors from the neighboring terminals E, B, A, F, D, and G.

Next section proposes a technique to implement the PLNC described above. As is shown in Fig. 1, because the two-dimensional wireless network is symmetrical, all the relays can be swapped with the terminals. This means that signal processing needed at the terminals in the first slot is necessary at the relays in the second slot. In other words, transmission signal processing needed for the terminals in the first slot can be applied to the relays in the second slot to transmit the signals. Since the same signal processing is used in the first and the second slot, we explain the proposed technique for the first slot in the next section.

3.1 Multichannel Filtering

As is defined in (1), $3N_{\mathrm{T}}$ signals are received at every relay. This section proposes multi-input physical layer network coding where the received signals coming from the three neighbors are detected as $3N_{\mathrm{S}}$ XOR-coded signals. The proposed multi-input PLNC applies multichannel filtering to get those XOR-coded signals. The multichannel filtering introduces some spatial filters at the relays. For example, the relay R_2 is introduced spatial filters $W_{2\mathrm{E}} \in \mathbb{C}^{N_{\mathrm{S}}\times N_{\mathrm{R}}}$, $W_{2\mathrm{C}} \in \mathbb{C}^{N_{\mathrm{S}}\times N_{\mathrm{R}}}$, and $W_{2\mathrm{B}} \in \mathbb{C}^{N_{\mathrm{S}}\times N_{\mathrm{R}}}$ that satisfy the following characteristics, $W_{2\mathrm{E}}\dot{H}_{2\mathrm{E}} = W_{2\mathrm{C}}\dot{H}_{2\mathrm{C}} = W_{2\mathrm{B}}\dot{H}_{2\mathrm{B}} = O_{N_{\mathrm{S}}\times N_{\mathrm{T}}}$ where $O_{n\times m} \in \mathbb{C}^{n\times m}$ indicates the null matrix of size $n \times m$. When the spatial filters $W_{2\mathrm{E}}$, $W_{2\mathrm{C}}$, and $W_{2\mathrm{B}}$ are applied to the relay R_2, the received signal vector $\dot{Y}_2$ is transformed to the vectors $Y_{2\mathrm{BC}} \in \mathbb{C}^{N_{\mathrm{S}}}$, $Y_{2\mathrm{BE}} \in \mathbb{C}^{N_{\mathrm{S}}}$, and $Y_{2\mathrm{CE}} \in \mathbb{C}^{N_{\mathrm{S}}}$, which are written as,

$$Y_{2\mathrm{BC}} = W_{2\mathrm{E}}\dot{Y}_2 = W_{2\mathrm{E}}\dot{H}_{2\mathrm{B}}X_{\mathrm{B}} + W_{2\mathrm{E}}\dot{H}_{2\mathrm{C}}X_{\mathrm{C}} + N_{2\mathrm{E}} \quad (3)$$

$$Y_{2\mathrm{BE}} = W_{2\mathrm{C}}\dot{Y}_2 = W_{2\mathrm{C}}\dot{H}_{2\mathrm{B}}X_{\mathrm{B}} + W_{2\mathrm{C}}\dot{H}_{2\mathrm{E}}X_{\mathrm{E}} + N_{2\mathrm{C}} \quad (4)$$

$$Y_{2\mathrm{CE}} = W_{2\mathrm{B}}\dot{Y}_2 = W_{2\mathrm{B}}\dot{H}_{2\mathrm{C}}X_{\mathrm{C}} + W_{2\mathrm{B}}\dot{H}_{2\mathrm{E}}X_{\mathrm{E}} + N_{2\mathrm{B}} \quad (5)$$

In the above equations, $N_{2\mathrm{E}} \in \mathbb{C}^{N_{\mathrm{S}}}$, $N_{2\mathrm{C}} \in \mathbb{C}^{N_{\mathrm{S}}}$, and $N_{2\mathrm{B}} \in \mathbb{C}^{N_{\mathrm{S}}}$ denote spatial filtered noise vectors defined as $N_{2\mathrm{E}} = W_{2\mathrm{E}}\dot{N}_2$, $N_{2\mathrm{C}} = W_{2\mathrm{C}}\dot{N}_2$, and $N_{2\mathrm{B}} = W_{2\mathrm{B}}\dot{N}_2$. The use of the multichannel filtering transforms the system model in (1) into that consisting of the three channels, which is the reason that the technique is named "multichannel filtering" in this paper. If we combine those transformed received signal vectors $Y_{2\mathrm{BC}}$, $Y_{2\mathrm{BE}}$, and $Y_{2\mathrm{CE}}$ into a composite received vector $Y_2 \in \mathbb{C}^{3N_{\mathrm{S}}}$, the composite received vector Y_2 can be written as follows.

$$Y_2 = \begin{bmatrix} Y_{2\mathrm{BC}} \\ Y_{2\mathrm{BE}} \\ Y_{2\mathrm{CE}} \end{bmatrix} = \begin{bmatrix} W_{2\mathrm{E}}\dot{H}_{2\mathrm{B}} & W_{2\mathrm{E}}\dot{H}_{2\mathrm{C}} & O_{N_{\mathrm{S}}\times N_{\mathrm{T}}} \\ W_{2\mathrm{C}}\dot{H}_{2\mathrm{B}} & O_{N_{\mathrm{S}}\times N_{\mathrm{T}}} & W_{2\mathrm{C}}\dot{H}_{2\mathrm{E}} \\ O_{N_{\mathrm{S}}\times N_{\mathrm{T}}} & W_{2\mathrm{B}}\dot{H}_{2\mathrm{C}} & W_{2\mathrm{B}}\dot{H}_{2\mathrm{E}} \end{bmatrix} \begin{bmatrix} X_{\mathrm{B}} \\ X_{\mathrm{C}} \\ X_{\mathrm{E}} \end{bmatrix} + \begin{bmatrix} N_{2\mathrm{E}} \\ N_{2\mathrm{C}} \\ N_{2\mathrm{B}} \end{bmatrix} \quad (6)$$

As is seen in (6), since every element of the vector Y_2 is a sum of the two vectors and the noise, the XOR-coded signals $d_{2\mathrm{CE}}$, $d_{2\mathrm{BC}}$, and $d_{2\mathrm{BE}}$ can be estimated with the maximum likelihood detection [2]. The following section proposes a technique to generate those spatial filters for the proposed PLNC.

3.2 Spatial Filters For Multichannel Filtering

First of all, precoding with a precoding matrix $\Psi \in \mathbb{C}^{N_{\mathrm{T}}\times N_{\mathrm{A}}}$ is applied to all the terminals, which transforms the channel matrix into an equivalent channel matrix where $N_{\mathrm{A}} \in \mathbb{N}$ represents the number of an equivalent transmit antennas. For example, the channel matrix $\dot{H}_{n\Omega} \in \mathbb{C}^{N_{\mathrm{R}}\times N_{\mathrm{T}}}$ between the relay R_n and the terminal Ω is transformed as,

$$H_{n\Omega} = \dot{H}_{n\Omega}\Psi. \quad (7)$$

$H_{n\Omega} \in \mathbb{C}^{N_{\mathrm{R}}\times N_{\mathrm{A}}}$ denotes an equivalent channel matrix. The number of the equivalent transmit antennas N_{A} is set as $N_{\mathrm{R}} > N_{\mathrm{A}}$, even if N_{T} is greater than N_{R}. The precoding enables the equivalent channel matrix $H_{\mathrm{n}\Omega}$ to be singular value decomposed as,

$$H_{n\Omega} = \begin{bmatrix} U_{n\Omega} & \widetilde{U}_{n\Omega} \end{bmatrix} \begin{bmatrix} \Gamma_{n\Omega} \\ O_{(N_{\mathrm{R}}-N_{\mathrm{A}})\times N_{\mathrm{A}}} \end{bmatrix} V_{n\Omega}^{\mathrm{H}} \quad (8)$$

In the above equation, superscript H, $\begin{bmatrix} U_{n\Omega} & \widetilde{U}_{n\Omega} \end{bmatrix} \in \mathbb{C}^{N_{\mathrm{R}}\times N_{\mathrm{R}}}$, $V_{n\Omega} \in \mathbb{C}^{N_{\mathrm{A}}\times N_{\mathrm{A}}}$, and $\Gamma_{n\Omega} \in \mathbb{C}^{N_{\mathrm{A}}\times N_{\mathrm{A}}}$ represent Hermitian transpose of a matrix or a vector, unitary matrices and a diagonal matrix. In addition, $U_{n\Omega} \in \mathbb{C}^{N_{\mathrm{R}}\times N_{\mathrm{A}}}$ and $\widetilde{U}_{n\Omega} \in \mathbb{C}^{N_{\mathrm{R}}\times(N_{\mathrm{R}}-N_{\mathrm{A}})}$ denote submatrices of the unitary matrix. The number of the streams N_{S} is defined as $N_{\mathrm{S}} = N_{\mathrm{R}} - N_{\mathrm{A}}$. $U_{n\Omega}$ is a submatrix corresponding to the diagonal matrix $\Gamma_{n\Omega}$, and $\widetilde{U}_{n\Omega}$ is the submatrix corresponding to the null matrix. Therefore, the spatial filter $W_{n\Omega}$ can be obtained as follows.

$$W_{n\Omega} = \widetilde{U}_{n\Omega}^{\mathrm{H}} \quad (9)$$

3.3 Precoding For System With Multichannel Filtering

Even if the multichannel filtering is employed in the system, the two signal vectors are simultaneously received at each channel. To simplify the signal defection in the channels, we apply precoding for the channels with multichannel filtering. For deriving the precoding, the system model in (6) is rewritten with multichannel filtering as,

$$Y_n = S_{n\Omega_1} + S_{n\Omega_2} + S_{n\Omega_3} + N_n, \quad (10)$$

where $S_{n\Omega_1} \in \mathbb{C}^{3N_{\mathrm{S}}}$, $S_{n\Omega_2} \in \mathbb{C}^{3N_{\mathrm{S}}}$, and $S_{n\Omega_3} \in \mathbb{C}^{3N_{\mathrm{S}}}$ represent arrival signal vectors sent by the terminals Ω_1, Ω_2, and Ω_3. $N_n \in \mathbb{C}^{3N_{\mathrm{S}}}$ is a composite AWGN vector defined as $N_n = \begin{bmatrix} N_{n\Omega_1}^{\mathrm{T}} & N_{n\Omega_2}^{\mathrm{T}} & N_{n\Omega_3}^{\mathrm{T}} \end{bmatrix}^{\mathrm{T}}$. Those arrival signal vectors are defined in the following.

$$S_{n\Omega_1} = \begin{bmatrix} W_{n\Omega_3}H_{n\Omega_1} \\ W_{n\Omega_2}H_{n\Omega_1} \\ O_{N_{\mathrm{S}}\times N_{\mathrm{T}}} \end{bmatrix} X_{\Omega_1} \quad (11)$$

$$S_{n\Omega_2} = \begin{bmatrix} W_{n\Omega_3}H_{n\Omega_2} \\ O_{N_{\mathrm{S}}\times N_{\mathrm{T}}} \\ W_{n\Omega_1}H_{n\Omega_2} \end{bmatrix} X_{\Omega_2} \quad (12)$$

$$S_{n\Omega_3} = \begin{bmatrix} O_{N_{\mathrm{S}}\times N_{\mathrm{T}}} \\ W_{n\Omega_2}H_{n\Omega_3} \\ W_{n\Omega_1}H_{n\Omega_3} \end{bmatrix} X_{\Omega_3} \quad (13)$$

As is shown, those arrival vectors have a null matrix. While the null matrices are very important to describe the system model, the null matrices do not need to be taken into account from the view point of precoder design. We define component signal vectors where the null matrices are removed, i.e., $\dot{S}_{n\Omega_1} = \left[(W_{n\Omega_3}H_{n\Omega_1})^{\mathrm{T}}\ (W_{n\Omega_2}H_{n\Omega_1})^{\mathrm{T}}\right]^{\mathrm{T}} X_{\Omega_1} \in \mathbb{C}^{2N_{\mathrm{S}}}$, $\dot{S}_{n\Omega_2} = \left[(W_{n\Omega_3}H_{n\Omega_2})^{\mathrm{T}}\ (W_{n\Omega_1}H_{n\Omega_2})^{\mathrm{T}}\right]^{\mathrm{T}} X_{\Omega_2} \in \mathbb{C}^{2N_{\mathrm{S}}}$, and $\dot{S}_{n\Omega_3} = \left[(W_{n\Omega_2}H_{n\Omega_3})^{\mathrm{T}}\ (W_{n\Omega_1}H_{n\Omega_3})^{\mathrm{T}}\right]^{\mathrm{T}} X_{\Omega_3} \in \mathbb{C}^{2N_{\mathrm{S}}}$. On the other hand, the transmission signal vector sent by the terminal Ω arrives not only at the relay R_n but also at the other neighboring relays in the first slot. For example, the signal vector sent by the terminal C reach the relays R_2, R_3, and R_4, as shown in Fig. 1. We have to apply the precoding to simplify the signal detection at all the neighboring nodes such as the relays R_2, R_3, and R_4. A composite arrival signal vector that has traveled in the fading channel from the terminal Ω to the relays R_{n_1}, R_{n_2}, and R_{n_3} is defined as follows,

$$S_\Omega = \begin{bmatrix} \dot{S}_{n_1\Omega} \\ \dot{S}_{n_2\Omega} \\ \dot{S}_{n_3\Omega} \end{bmatrix} = \begin{bmatrix} W_{n_1\Omega_1}H_{n_1\Omega} \\ W_{n_1\Omega_2}H_{n_1\Omega} \\ W_{n_2\Omega_3}H_{n_2\Omega} \\ W_{n_2\Omega_4}H_{n_2\Omega} \\ W_{n_3\Omega_5}H_{n_3\Omega} \\ W_{n_3\Omega_6}H_{n_3\Omega} \end{bmatrix} X_\Omega = H_\Omega X_\Omega \tag{14}$$

In (14), $S_\Omega \in \mathbb{C}^{6N_{\mathrm{S}}}$ and $H_\Omega \in \mathbb{C}^{6N_{\mathrm{S}}\times N_{\mathrm{A}}}$ denote the composite arrival signal vector and a composite filtered channel matrix defined as $H_\Omega = \left[(W_{n_1\Omega_{m_1}}H_{n_1\Omega})^{\mathrm{T}}\ (W_{n_1\Omega_{m_2}}H_{n_1\Omega})^{\mathrm{T}}\ \ldots\ (W_{n_3\Omega_{m_3}}H_{n_3\Omega})^{\mathrm{T}}\right]^{\mathrm{T}}$. A non-linear precoding is applied to the system model defined in (14) for higher transmission performance and reduction of the signal detection complexity. This paper uses MMSE-based non-linear precoding, which is defined as [12],

$$X_\Omega = g_\Omega F_\Omega^{\mathrm{H}} v_\Omega \tag{15}$$

$F_\Omega \in \mathbb{C}^{6N_{\mathrm{S}}\times N_{\mathrm{A}}}$, $g_\Omega \in \mathbb{R}$, and $v_\Omega \in \mathbb{C}^{6N_{\mathrm{S}}}$ in (15) indicate a feed forward filter matrix, a normalization factor, and a feed back filter output vector. The feed forward filter is defined as,

$$F_\Omega^{\mathrm{H}} = H_\Omega^{\mathrm{H}} P_\Omega^{\mathrm{T}} L_\Omega^{\mathrm{H}} \Gamma_\Omega \tag{16}$$

$$P_\Omega \left(H_\Omega H_\Omega^{\mathrm{H}} + \frac{6N_{\mathrm{S}}\sigma^2}{P} I_{6N_{\mathrm{S}}}\right)^{-1} P_\Omega^{\mathrm{T}} = L_\Omega^{\mathrm{H}} \Gamma_\Omega L_\Omega, \tag{17}$$

where $P_\Omega \in \mathbb{C}^{6N_{\mathrm{S}}\times 6N_{\mathrm{S}}}$, $\Gamma_\Omega \in \mathbb{C}^{6N_{\mathrm{S}}\times 6N_{\mathrm{S}}}$, $L_\Omega \in \mathbb{C}^{6N_{\mathrm{S}}\times 6N_{\mathrm{S}}}$, $\sigma^2 \in \mathbb{R}$ and $P \in \mathbb{R}$ denote a permutation matrix, a diagonal matrix, a lower triangular matrix with one in the diagonal positions, a variance of AWGN and the transmission power. In addition, I_n indicates the n-dimensional identity matrix. The feed back filter output vector v_Ω can be defined with the lower triangular matrix and the permutation matrix.

$$v_\Omega = L_\Omega \left(P_\Omega D_\Omega + k_\Omega M_\Omega\right) \tag{18}$$

In the above equation, $D_\Omega \in \mathbb{C}^{6N_{\mathrm{S}}}$, $k_\Omega \in \mathbb{C}^{6N_{\mathrm{S}}\times 6N_{\mathrm{S}}}$, and $M_\Omega \in \mathbb{R}^{6N_{\mathrm{S}}}$ represent a modulation signal vector, a diagonal matrix with Gaussian integers in the diagonal positions, and a modulus vector. They are defined as $D_\Omega = \left[d_{n_1\Omega}^{\mathrm{T}}\ d_{n_1\Omega}^{\prime\,\mathrm{T}} \cdots d_{n_3\Omega}^{\prime\,\mathrm{T}}\right]^{\mathrm{T}}$, $k_\Omega = \mathrm{diag}\left(k_{n_1\Omega}\ k'_{n_1\Omega} \cdots k'_{n_3\Omega}\right)$, and $M_\Omega = \left[\ M_{n_1\Omega}^{\mathrm{T}}\ M_{n_1\Omega}^{\prime\,\mathrm{T}} \cdots M_{n_3\Omega}^{\prime\,\mathrm{T}}\ \right]^{\mathrm{T}}$, where $d_{n_i\Omega} \in \mathbb{C}^{N_{\mathrm{S}}}$ and $d'_{n_i\Omega} \in \mathbb{C}^{N_{\mathrm{S}}}$ denote transmission signal vectors sent from the terminal Ω to the two terminals neighboring to the relay n_i, respectively. $k_{n_i\Omega} \in \mathbb{C}^{N_{\mathrm{S}}\times N_{\mathrm{S}}}$ and $k'_{n_i\Omega} \in \mathbb{C}^{N_{\mathrm{S}}\times N_{\mathrm{S}}}$ represent the Gaussian integer matrices for $d_{n_i\Omega}$ and $d'_{n_i\Omega}$. While the modulus vector is defined in the next section, the Gaussian integer matrix is obtained with a vector modulo function Mod[] to improve the transmission performance,

$$v_\Omega = \mathrm{Mod}\left[P_\Omega D_\Omega - B_\Omega v_\Omega, M_\Omega\right], \tag{19}$$

where $B_\Omega \in \mathbb{C}^{6N_{\mathrm{S}}\times 6N_{\mathrm{S}}}$ denotes a lower triangular matrix defined as $B_\Omega = L_\Omega^{-1} - I_{6N_{\mathrm{S}}}$. Let $\mathrm{Re}[c] \in \mathbb{R}$, $\mathrm{Im}[c] \in \mathbb{R}$, $U \in \mathbb{C}^N$ and $M \in \mathbb{R}^N$ represent a real part and an imaginary part of a complex vectors c, a complex vector, and a real vector, the vector modulo function is defined as $\mathrm{Mod}\left[U, M\right] = [\mathrm{cmod}(u(1), M(1))\ \mathrm{cmod}(u(2), M(2))\ \cdots\ \mathrm{cmod}(u(N), M(N))]^{\mathrm{T}}$ where $u(i) \in \mathbb{C}$, $M(i) \in \mathbb{R}$, and $\mathrm{cmod}\left(u(i), M(i)\right)$ indicate an ith entry of a vector U, an ith entry of a vector M and a complex modulo function defined as $\mathrm{cmod}\left(u(i), M(i)\right) = \mathrm{mod}\left(\mathrm{Re}\left[u(i), M(i)\right]\right) + \mathrm{j} \cdot \mathrm{mod}\left(\mathrm{Im}\left[u(i), M(i)\right]\right)$. On the other hand, the normalization factor is defined to set the average transmission power to P as follows,

$$g_\Omega = \sqrt{\frac{P}{\mathrm{tr}[R_\Omega F_\Omega F_\Omega^{\mathrm{H}}]}}, \tag{20}$$

where $\mathrm{tr}[\Lambda]$ and $R_\Omega \in \mathbb{C}^{6N_{\mathrm{S}}\times 6N_{\mathrm{S}}}$ represent a trace of a matrix Λ and a correlation matrix of the feed back filter output vector v_Ω defined as $R_\Omega = \mathrm{E}[v_\Omega v_\Omega^{\mathrm{H}}]$. When the non-linear MMSE precoder defined in (15) is applied at the terminal Ω, the composite signal vector defined in (14) can be approximately rewritten as,

$$S_\Omega \simeq \begin{bmatrix} \dot{S}_{n_1\Omega} \\ \dot{S}_{n_2\Omega} \\ \dot{S}_{n_3\Omega} \end{bmatrix} = g_\Omega (D_\Omega + k_\Omega M_\Omega) \tag{21}$$

As is defined previously, the $\dot{S}_{n_1\Omega}$ is the received signal vector sent from the terminal Ω to the relay R_{n_1} in the first slot. The equation (21) implies that the proposed precoder enables the terminal Ω to deliver only the signals of interest to the relay R_{n_1}, i.e., $\dot{S}_{n_1\Omega} = g_\Omega \left(\left(d_{n_1\Omega}^{\mathrm{T}}\ d_{n_1\Omega}^{\prime\,\mathrm{T}}\right)^{\mathrm{T}} + \left(\left(k_{n_1\Omega}\ M_{n_1\Omega}\right)^{\mathrm{T}}\ \left(k'_{n_1\Omega}\ M'_{n_1\Omega}\right)^{\mathrm{T}}\right)^{\mathrm{T}}\right)$. Next section explains the optimum modulus vector setting that maximizes the transmission performance.

3.4 Modulus Setting

As is described in the paragraph above (14), the component signal vector $\dot{S}_{n\Omega}$ is a sub vector of the arrival signal vector $S_{n\Omega}$. Since the component signal vector $\dot{S}_{n\Omega}$ can be expressed as $\dot{S}_{n\Omega} = g_\Omega \left(\left(d_{n\Omega}^{\mathrm{T}} \; d_{n\Omega}'^{\mathrm{T}} \right)^{\mathrm{T}} + \left((k_{n\Omega} M_{n\Omega})^{\mathrm{T}} \; \left(k'_{n\Omega} \, M'_{n\Omega} \right)^{\mathrm{T}} \right)^{\mathrm{T}} \right)$ by using the proposed precoding, the arrival vector $S_{n\Omega}$ can be written as, for example,

$$S_{n\Omega} = g_\Omega \begin{bmatrix} d_{n\Omega} + k_{n\Omega} M_{n\Omega} \\ d'_{n\Omega} + k'_{n\Omega} M'_{n\Omega} \\ 0 \end{bmatrix}. \tag{22}$$

If the arrival signal vectors $S_{n\Omega_1}$, $S_{n\Omega_2}$, and $S_{n\Omega_3}$ written like in (22) are substituted for (11)~(13), the composite received signal vector Y_n in (10) can be rewritten as,

$$\begin{aligned} Y_n &= \begin{bmatrix} Y_{n\Omega_1\Omega_2} \\ Y_{n\Omega_1\Omega_3} \\ Y_{n\Omega_2\Omega_3} \end{bmatrix} \\ &= \begin{bmatrix} g_{\Omega_1} d_{n\Omega_1} + g_{\Omega_2} d_{n\Omega_2} + (g_{\Omega_1} k_{n\Omega_1} M_{n\Omega_1} + g_{\Omega_2} k_{n\Omega_2} M_{n\Omega_2}) \\ g_{\Omega_1} d'_{n\Omega_1} + g_{\Omega_3} d_{n\Omega_3} + (g_{\Omega_1} k'_{n\Omega_1} M'_{n\Omega_1} + g_{\Omega_3} k_{n\Omega_3} M_{n\Omega_3}) \\ g_{\Omega_2} d'_{n\Omega_2} + g_{\Omega_3} d'_{n\Omega_3} + (g_{\Omega_2} k'_{n\Omega_2} M'_{n\Omega_2} + g_{\Omega_3} k'_{n\Omega_3} M'_{n\Omega_3}) \end{bmatrix} \\ &\quad + \begin{bmatrix} N_{n\Omega_3} \\ N_{n\Omega_2} \\ N_{n\Omega_1} \end{bmatrix} \end{aligned} \tag{23}$$

Not only the modulation signal vectors but also the Gaussian integer multiples of the modulus vectors are contained in the composite received signal vector Y_n as well as the noise vector. The Gaussian integer multiples have to be removed to detect the modulation signal vectors D_{Ω_m} $m = 1, 2, 3$. Because the Gaussian integer matrices are determined independently at the precoders, the Gaussian integer multiples $k_{n\Omega} M_{n\Omega}$ are randomly varied. To remove the Gaussian integer multiples, for example, the modulus in the first row of (23) has to be set to satisfy the following requirement.

$$g_{\Omega_1} M_{n\Omega_1} = g_{\Omega_2} M_{n\Omega_2} = M_{n\Omega_1\Omega_2} \tag{24}$$

In (24), $M_{n\Omega_1\Omega_2} \in \mathbb{R}$ denotes a modulus that is used to remove the Gaussian integer multiples at the relay R_n in the first slot. When the quaternary phase sift keying (QPSK) is applied to the system, the Gaussian integer multiples can be successfully removed by setting the modulus vector $M_{n\Omega_1\Omega_2}$ to satisfy the following [2], [11].

$$M_{n\Omega_1\Omega_2} = 2(g_{\Omega_1} + g_{\Omega_2}) \tag{25}$$

Hence, the modulus for the non-linear precoding can be obtained as,

$$\begin{aligned} M_{n\Omega_1} &= 2(1 + g_{\Omega_2}/g_{\Omega_1}), \quad M'_{n\Omega_1} = 2(1 + g_{\Omega_3}/g_{\Omega_1}) \\ M_{n\Omega_2} &= 2(1 + g_{\Omega_1}/g_{\Omega_2}), \quad M'_{n\Omega_2} = 2(1 + g_{\Omega_3}/g_{\Omega_2}) \\ M_{n\Omega_3} &= 2(1 + g_{\Omega_1}/g_{\Omega_3}), \quad M'_{n\Omega_3} = 2(1 + g_{\Omega_2}/g_{\Omega_3}) \end{aligned} \tag{26}$$

By performing the modulo operation in each channel with the modulus, we can successfully remove the Gaussian integer multiples as,

$$\begin{aligned} \bar{Y}_n &= \begin{bmatrix} \mathrm{Mod}(Y_{n\Omega_1\Omega_2}, M_{n\Omega_1\Omega_2}) \\ \mathrm{Mod}(Y_{n\Omega_1\Omega_3}, M_{n\Omega_1\Omega_3}) \\ \mathrm{Mod}(Y_{n\Omega_2\Omega_3}, M_{n\Omega_2\Omega_3}) \end{bmatrix} \\ &= \begin{bmatrix} g_{\Omega_1} d_{n\Omega_1} + g_{\Omega_2} d_{n\Omega_2} + N_{n\Omega_3} \\ g_{\Omega_1} d'_{n\Omega_1} + g_{\Omega_3} d_{n\Omega_3} + N_{n\Omega_2} \\ g_{\Omega_2} d'_{n\Omega_2} + g_{\Omega_3} d'_{n\Omega_3} + N_{n\Omega_1} \end{bmatrix}, \end{aligned} \tag{27}$$

where $\bar{Y}_n \in \mathbb{C}^{6N_\mathrm{S}}$ denotes a received signal vector free from the Gaussian integer multiples. Because the factors $g_{\Omega_1} \sim g_{\Omega_3}$ are all real, we can obtain the XOR-coded signals by means of the region detection technique [2]. For example, the relay R_2 gets the XOR-coded signal vector as,

$$D_2 = \begin{bmatrix} d_{2\mathrm{B}} \oplus d_{2\mathrm{C}} \\ \vdots \\ d'_{2\mathrm{C}} \oplus d'_{2\mathrm{E}} \end{bmatrix} = \mathrm{rdet}\left[\; Y_2 \; \right] \tag{28}$$

where rdet[] indicates a region detection function implemented with slicers. While the XOR-coded vectors have to be obtained at the relays in the first slot, all the modulation signal vectors have to be detected at the terminals in the second slot. The maximum likelihood (MLD) is used for the signal detection at the terminals in the second slot.

Because the region detection can be used for the XOR-coding as a kind of signal detection at the relays, only the small computational complexity is imposed on the relays. On the other hand, when the MLD is used at the terminals for the signal detection in the second slot, the computational complexity imposed on the terminals becomes more than that on the relays. Because the proposed precoding transforms the system model into that with a real channel gain as shown in (27), however, the MLD can be implemented with much less computational complexity than the original MLD. Since the received signals are a real valued weight sum of the two signals except for the AWGN, the number of the complex multiplications is only $24N_\mathrm{S}$ to detect the signals in the system defined in (27). The number of the complex multiplications for the signal detection is much less than that needed in the original MLD, i.e., about $18N_\mathrm{S}^2 4^{6N_\mathrm{S}}$.

3.5 Summary of Proposed Multi-Input PLNC

The proposed multi-input PLNC for the signal exchange among the neighboring terminals in the two-dimensional networks is summarized as follows.

1st time slot: Terminals transmit packets for relays

1. linear channel precoding with a matrix Ψ
2. singular value decomposition of equivalent channels
3. non linear precoding with composite filtered channel matrices
4. XOR-coding as signal detection at relays

2nd time slot: Relays transmit packets for terminals

1. linear channel precoding with a matrix Ψ

2. singular value decomposition of equivalent channels
3. non linear precoding with composite filtered channel matrices
4. MLD after modulo operation
5. XOR-operation with own signals to detect signals

Even though N_T and N_R antennas are placed on the terminals and the relays respectively, the multichannel filtering reduces the size of the received signal vector to that of the composite received signal vector $\dot{Y}_n$, i.e., $3N_S$ as is defined above (6). The composite received signal vector consists of the three transformed signal vectors $Y_{n\Omega_1\Omega_2}$ with the size of N_S. The precoder makes the terminal send the signal vector with the size of N_S to the relay R_2 in the 1st slot. Because the two signal vectors with the size of NS are contained in one transformed signal vector, the total number of the transmission signals in the composite received signal vector is $6N_S$, i.e., $3 \times N_S \times 2$. In a word, $6N_S$ transmission signals are contained in the composite received signal vector. Since the same signal processing is performed in the 1st and the 2nd slot, the composite received signal vector containing $6N_S$ transmission signals is also received at the terminal in the 2nd slot. The MLD is performed with the composite received signal vector to detect the $6N_S$ transmission signals. The decoding defined in (2) is carried out with the detected signals at the terminals to get the transmission signals sent by the neighbors.

4. Computer Simulation

The transmission performance of the proposed multi-input PLNC is evaluated by computer simulation. Block Rayleigh fading is applied to channel models between all the antennas on the relays and those on the terminals. As is described, the QPSK modulation is used. The two-dimensional multihop network shown in Fig. 1 is used for the performance evaluation†. Table 1 shows the simulation parameters. All the transmitters and the relays are perfectly timing-synchronized††. If the number of the antennas on the terminal is greater than that on the relay, i.e., $N_T > N_R$, we use a precoding matrix Ψ defined as $\Psi = \begin{bmatrix} I_{N_A} & O_{N_A\times(N_T-N_A)} \end{bmatrix}^T$ in the first slot and $\Psi = I_{N_R}$ in the second slot. On the other hand, if the number of the antennas on the terminal is not more than that on the receiver, i.e., $N_T \le N_R$, we use a matrix defined as $\Psi = I_{N_T}$ in the first slot and $\Psi = \begin{bmatrix} I_{N_A} & O_{N_A\times(N_R-N_A)} \end{bmatrix}^T$ in the second slot†††.

Table 1 Simulation parameters.

Channel model	Rayleigh fading
Modulation scheme	QPSK
Number of antennas on terminals N_T	6, 7, 8, 14
Number of antennas on relays N_R	6, 7, 8, 14
Number of streams of transmitted signals N_S	1, 2
Channel coding	N.A.

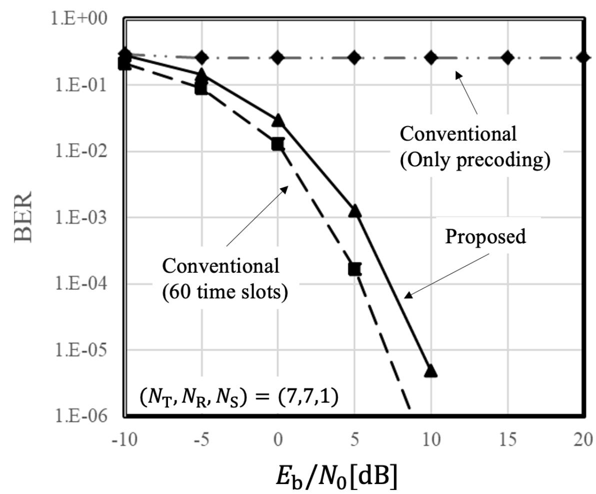

Fig. 2 Transmission performance of proposed PLNC at relays.

4.1 Comparison With Conventional Techniques

Figure 2 compares the transmission performance of the proposed PLNC with conventional techniques at the relays in the 1st slot. The vertical axis is the average bit error rate (BER), and the horizontal axis is the energy per bit to noise power spectral density ratio (E_b/N_0). The number of the antennas on the terminal and that on the relay are 7 and 7, i.e., $N_T = N_R = 7$. N_S is set to 1. In the figure, the proposed PLNC is compared with two conventional techniques. One of them is an access control based technique that allows only one terminal to send the packets to the relays among the three neighboring terminals in the first slot, and that does only one relay to send in the second slot. This technique is referred as "60 time slots" in the figure. The other technique is only the MMSE-based precoding applied at the transmitters, which is referred as "only precoding". As is implied above, the proposed PLNC is compared with

† While conventional two-input PLNCs can be implemented for high throughput in square or triangle multihop networks, they are not effective in hexagonal multihop networks. The multi-input PLNC is proposed to improve the throughput in such hexagonal multihop networks. The multi-input PLNC in more complicated multihop networks is also one of our future works.

†† The proposed PLNC is degraded due to the timing synchronization error as other decode and forward PLNCs, while the performance degradation depends on modulation schemes and filters used in systems. Because many network synchronization techniques have been investigated such as GPS based techniques, namely, IEEE-1588, we think that some of them could be applied to our proposed system. Anyway, synchronization for the proposed PLNC is one of our future works.

††† While the system model for the signal transmission in the first slot is defined in (1), the system model in the second slot is described as $\dot{Y}_\Omega = \dot{H}^H_{n_1\Omega}X_{n_1} + \dot{H}^H_{n_2\Omega}X_{n_2} + \dot{H}^H_{n_3\Omega}X_{n_3} + \dot{N}_\Omega$ where $\dot{Y}_\Omega \in \mathbb{C}^{N_T}$, $X_{n_m} \in \mathbb{C}^{N_R}$, and $\dot{N}_\Omega \in \mathbb{C}^{N_T}$ denote a signal vector received at the terminal Ω, a transmission signal vector from the relay R_{n_m}, and the AWGN vector at the terminal Ω. The size of the linear precoder matrix Ψ is changed adjust to the transmission signal vector size.

those conventional techniques in the same situation i.e., the hexagonal network where N_T antennas and N_R antennas are placed on each terminal and relay respectively. Because the "60 time slot" technique makes interference free transmission, the technique applies the non-linear precoding defined in (15) ~ (20) for fair comparison. However, if the multichannel filtering is not applied, the system model remains as the 7×7 MIMO system. The channel matrix H_Ω is replaced with the channel matrix $\dot{H}_{n\Omega}$ in the non-linear precoding for the "60 time slot" technique.

Because the 60 time slot technique makes the signal transmission interference-free, the technique achieves the performance upper bound. The 60 time slot technique delivers 7 signals to the neighboring terminal, while only 1 signal is sent to the neighboring terminal in the system with the proposed multi-input PLNC. When the 60 time slot technique is used, however, it takes 60 time slots for all the terminals to exchange their packets with their neighbors, while it takes only two time slot for the proposed PLNC to make all the terminals exchange their packet with the neighbors. Hence, the proposed PLNC achieves much higher frequency utilization efficiency than the 60 time slot technique. On the other hand, when the only MMSE precoding is used, the precoding has to be carried out for the system with the 3 neighbors. This means that the precoding has to be performed in the system with the channel matrix of $3N_R \times N_T$. To balance the transmission performance in the first slot and the second slot, the number of the relay antennas N_R should be not so different from that of the terminal antennas. In other words, $N_T \approx N_R$. If such parameter setting is applied, the conventional technique applies the MMSE precoding to very overloaded channels with the channel matrix of $3N_R \times N_T$. Therefore, the transmission performance is severely degraded. In contrast with them, the proposed PLNC achieves superior transmission performance while attaining high frequency utilization efficiency. As is shown in the figure, the performance gap from the upper bound is reduced to about 2 dB at the BER of 10^{-4}.

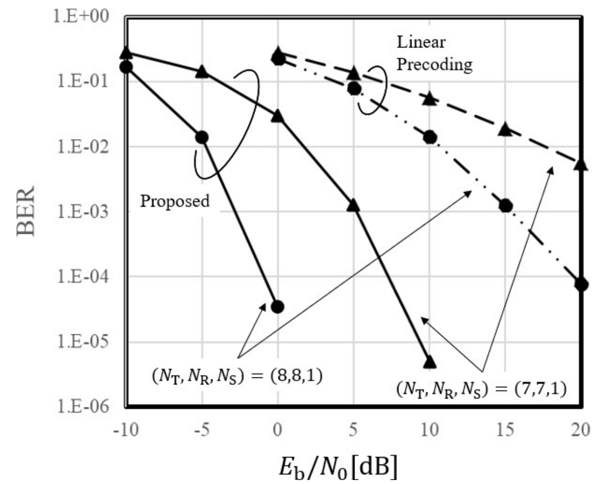

Fig. 3 Performance comparison with linear precoding at relays.

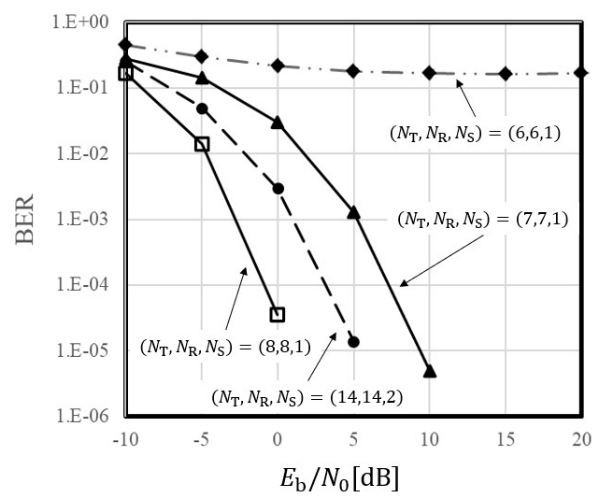

Fig. 4 Transmission performance of proposed PLNC at relays ($N_T = N_R$).

4.2 Comparison with Linear MMSE Precoding

Figure 3 compares the proposed PLNC and the PLNC with linear MMSE precoding in terms of the transmission performance at the relays. The proposed multichannel filtering is employed in the both PLNCs. (N_T, N_R, N_S) is set to $(7, 7, 1)$ and $(8, 8, 1)$. The number of the antennas on the terminal is the same to that on the relay. The proposed PLNC achieves 21 dB better transmission performance at the BER=10^{-4} than the PLNC with the linear precoding, when (N_T, N_R, N_S) is set to $(8, 8, 1)$.

4.3 Comparison with Different Transmit and Receive Antenna Combinations

As is shown previously, the number of the transmission signal streams is $6N_S$ in spite of the number of the antennas in the proposed PLNC. This means that the number of the antennas can be changed regardless of the number of the transmission signal streams, $6N_S$. Fig. 4 shows the transmission performance with respect to the number of the antennas when the number of the antennas on the terminal is the same to that on the relay. The transmission performance is more improved as the number of the antennas increases when $N_S = 1$. Even if N_S is increased to 2, the proposed PLNC still keeps high transmission performance by doubling the number of the antennas. On the other hand, the performance is deteriorated when the number of the antennas is reduced to 6, even if N_S is set to 1. When N_S is equal to 1, the number of the equivalent transmission antennas N_A is reduced to 5, because $N_A = N_R - N_S$ as described above. This implies that the 6 signal streams are transmitted in the channel with the channel matrix size of 6×5, which is regarded as an overloaded channel. Because the MMSE precoding deteriorates the transmission performance in such overloaded channel, the transmission performance is much worse than that of the other techniques.

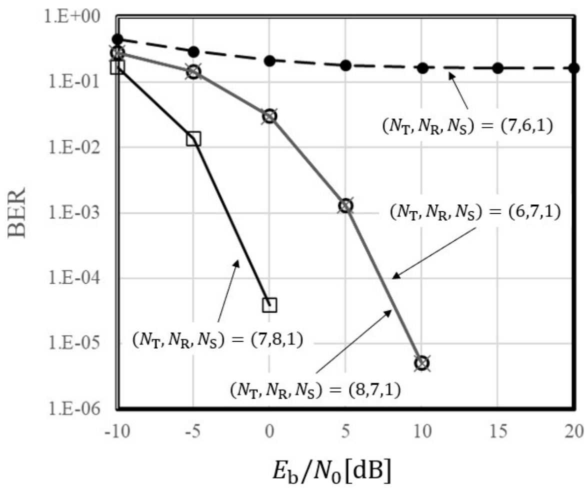

Fig. 5 Transmission performance of proposed PLNC at relays ($N_T \neq N_R$).

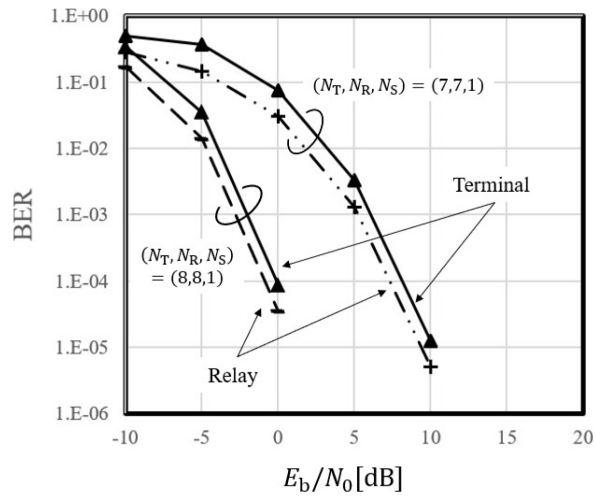

Fig. 6 Transmission performance at terminals ($N_T = N_R$).

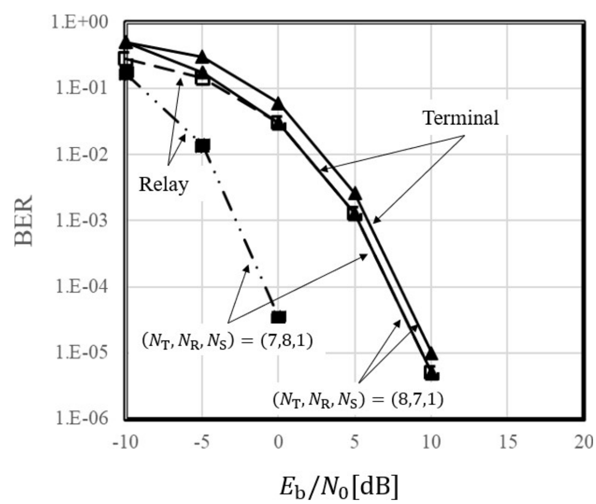

Fig. 7 Transmission performance at terminals ($N_T \neq N_R$).

Figure 5 shows the transmission performance of the proposed PLNC at the relay when the number of the antennas on the terminal is different from that on the relays. The proposed PLNC achieves better transmission performance as the number of the receive antennas increases in spite of the number of the transmit antennas. When the number of the antennas on the relay is 6, for example, the precoding with the precoding matrix Ψ reduces the number of the equivalent transmit antennas to 5, even though 7 antennas are put on the terminal. This causes the terminal to transmit 6 signal streams with 5 equivalent transmit antennas, which system is overloaded. The transmission performance is seriously degraded even if the proposed non-linear precoding is applied. When the number of the antennas on the relay is more than 6, the system is no longer overloaded. The higher diversity gain is attained as the number of the antennas on the relay increases.

4.4 Performance at Terminals

Figure 6 compares the transmission performance of the proposed PLNC at the terminal with that at the relay. The number of the relay antennas is the same to that of the terminal antennas in the figure. Because the almost same signal processing is carried out in the first slot and the second slot, the BER performance is about twice as much as that of the relay in spite of the number of the antennas†. The performance at the terminal is only less than 1 dB degraded from that of the relay in spite of the number of the antennas. Figure 7 also compares the transmission performance at the relay with that at the terminal when the number of the relay antennas is different from that of the terminal antennas. While the similar performance gap between the relay and the terminal can be seen when $(N_T, N_R, N_S) = (8, 7, 1)$, if the number of the relay antennas is increased, i.e., $(N_T, N_R, N_S) = (7, 8, 1)$, the transmission performance at the relay is improved. However, the transmission performance at the terminal is deteriorated. This means that the performance in the first slot is much better than that in the second slot. As is explained above, the transmission performance in the first slot depends on the number of the relay antennas. Besides, the performance in the second slot is dependent on the number of the terminal antennas due to the same reason. This is the reason that the transmission performance in the first slot is much better than that in the second slot. When the transmission performance in the second slot is worse than that in the first slot, the transmission performance at the terminals is deteriorated to that of the second slot, even if the transmission performance in the first slot is superb. Because the performance in the second slot depends on the number of the terminal antennas, therefor, the performance with $(7, 8, 1)$ becomes similar as that with $(8, 7, 1)$.

†When the conventional technique is applied, the same signal processing is exactly performed in the first and the second time slots. Therefore, the BER performance of the terminal is also about twice as much as that of the relay. The conventional technique achieves about 2 dB better performance than the proposed PLNC even at the terminals when the setting of $(N_T, N_R, N_S) = (7, 7, 1)$ is applied.

The above performance justifies the assumption that the signals transmitted from the vertices only arrive at those neighboring vertices as follows. Although the signal sent from the terminal A can arrive not only the relay R_3 but also at that R_2, for example, the received signal power is 12 dB lower than the power of the signal from C, B, E on average, because the pass loss exponent α is about 4 in wireless communication environment, if the relays are located beyond the breakpoints from the nearest terminals [19]. On the other hand, the multichannel filtering attains a gain of about 8.5 dB, and the precoding achieves the same gain when 7 antennas are placed at the relays and the terminals. Even though the three interference signals arrive at the receiver, hence, the SIR can be at most increased to about 24 dB. If the SIR performance is achieved, the proposed system can maintain the BER performance shown in the paper despite of the interference, because the required E_b/N_0 to achieve 10^{-6} is at most 15 dB. The signals from the terminal A can be neglected in the network†.

5. Conclusion

In this paper, we have proposed multi-input physical layer network coding (multi-input PLNC) for high speed wireless communication in two-dimensional multihop networks. In the proposed PLNC, all the terminals send their packets simultaneously for the neighboring relays to maximize the network throughput in the first slot, and all the relays also do for the neighboring terminal in the second slot. Those concurrent signal transmissions cause severe packet collisions at the relays and the terminals. To solve the difficulties caused by the packet collision, we propose multichannel filtering to reduce the number of the collision packets, which allows XOR-coding at the relays. A non-linear precoding is proposed for the proposed PLNC to simplify the signal detection at the relays and the terminals. The precoding makes it possible to detect XOR-coded signals with the region detection at the relays, and to reduce the detection complexity of the MLD at the terminals. The proposed multi-input PLNC makes all the terminals exchange their packets with the neighboring terminals in only two time slots. We also evaluated the BER performance of the proposed multi-input PLNC by computer simulation. The BER performance is improved as the number of the antennas increases when the number of the signal streams is kept constant. We have shown that the proposed PLNC achieves superior the BER performance if the number of the received antennas is more than that of the signal streams. The proposed PLNC with the non-linear precoding achieves 21 dB better transmission performance than the PLNC with linear precoding. The proposed PLNC can raise the frequency utilization efficiency despite of the superior transmission performance.

†Actually, since the performance could not be always achieved in real wireless environment, we have to consider another technique, which is one of our future works.

Acknowledgments

This work was supported by the JSPS KAKENHI JP21K04061 and support center for advanced telecommunications technology research (SCAT).

References

[1] R.H.Y. Louie, Y. Li, and B. Vucetic, "Practical physical layer network coding for two-way relay channels: Performance analysis and comparison," IEEE Trans. Wireless Commun., vol.9, no.2, pp.764–777, Feb. 2010.
[2] S. Denno, Y. Nagai, and Y. Hou, "XOR physical layer network coding with non-linear precoding for quadrature amplitude modulations in bi-directional MIMO relay systems," IEICE Trans. Wireless Commun., vol.E102-B, no.10, pp.2073–2081, Oct. 2019.
[3] M. Ju and I.M. Kim, "Error performance analysis of BPSK modulation in physical-layer network coded bi-directional relay networks," IEEE Trans. Commun., vol.58, no.10, pp.2770–2775, Sept. 2010.
[4] H. Gao, T. Lv, S. Zhang, C. Yuen, and S. Yang, "Zero-forcing based MIMO two-way relay with relay antenna selection: Transmission scheme and diversity analysis," IEEE Trans. Wireless Commun., vol.11, no.12, pp.4426–4437, Nov. 2012.
[5] M. Eslamifar, W.H. Chin, C. Yuen, and Y.L. Guan, "Performance analysis of two-step bi-directional relaying with multiple antennas," IEEE Trans. Wireless Commun., vol.11, no.12, pp.4237–4242, Nov. 2012.
[6] L. Shi, T. Yang, K. Cai, P. Chen, and T. Guo, "On MIMO linear physical layer network coding: Full-rate full-diversity design and optimization," IEEE Trans. Wireless Commun., vol.17, no.5, pp.3498–3511, March 2018.
[7] T.K. Akino, P. Popovski, and V. Tarokh, "Optimized constellations for two-way wireless relaying with physical network coding," IEEE J. Sel. Areas Commun., vol.27, no.5, pp.773–787, 2009.
[8] Y.T. Kim, K. Lee, M. Park, K.J. Lee, and I. Lee, "Precoding designs based on minimum distance for two-way relaying MIMO systems with physical network coding," IEEE Trans. Commun., vol.6, no.10, pp.4151–4160, Oct. 2013.
[9] S. Denno and D. Umehara, "Simplified maximum likelihood detection with unitary precoding for XOR physical layer network coding," IEICE Trans. Commun., vol.E100-B, no.1, pp.167–176, Jan. 2017.
[10] C. Lengchi and S. Denno, "Nonlinear precoding for XOR physical layer network coding in bi-directional MIMO relay systems," IEICE Trans. Commun., vol.E100-B, no.3, pp.440–448, March 2017.
[11] S. Denno, K. Yamamoto, and Y. Hou, "Precoded physical layer network coding with coded modulation in MIMO-OFDM bi-directional wireless relay systems," IEICE Trans. Commun., vol.E104-B, no.1, pp.99–101, Jan. 2021.
[12] K. Kusume, M. Joham, W. Utschick, and G. Bauch, "Cholesky factorization with symmetric permutation applied to detecting and precoding spatially multiplexed data streams," IEEE Trans. Wireless Commun., vol.55, no.6, pp.3089–3103, June 2007.
[13] G. Wang, W. Xiang, and J. Yuan, "Generalized wireless network coding schemes for multihop two-way relay channels," IEEE Trans. Wireless Commun., vol.13, no.9, pp.5132–5147, Sept. 2014.
[14] M. Peng, Q. Hu, X. Xie, Z. Zhao, and H.V. Poor, "Network coded multihop wireless communication networks: Channel estimation and training design," IEEE J. Sel. Areas Commun., vol.33, no.2, pp.281–294, Feb. 2015.
[15] H. Zhang and L. Cai, "Bi-directional multi-hop wireless pipeline using physical-layer network coding," IEEE Trans. Wireless Commun., vol.16, no.12, pp.7950–7965, Dec. 2017.
[16] K. Chi, X. Jiang, and S. Horiguchi, "Joint design of network coding and transmission rate selection for multihop wireless networks," IEEE Trans. Wireless Commun., vol.59, no.5, pp.2435–2444, June

2010.

[17] S. Lin and L. Fu, "Throughput capacity of IEEE 802.11 many-to/from-one bi-directional networks with physical-layer network coding," IEEE Trans. Wireless Commun., vol.15, no.1, pp.217–231, Jan. 2016.

[18] R.Y. Kim, J. Jin, and B. Li, "Scattered random network coding for efficient transmission in multihop wireless networks," IEEE Trans. Veh. Technol., vol.60, no.5, pp.2383–2389, June 2011.

[19] A. Karttunen, A.F. Molisch, S. Hur, J. Park, and C.J. Zhang, "Spatially consistent street-by-street path loss model for 28-GHz channels in micro cell urban environments," IEEE Trans. Wireless Commun., vol.16, no.11, pp.7538–7550, 2017.

Hideaki Tsugita received the B.S. and the M.S. degrees from Okayama University, Japan in 2020 and 2022, respectively. He has been engaged in the research of physical layer network coding. He is with Mitsubishi Electric Information Network by Digital Technology, Co., Ltd.

Satoshi Denno received the M.E. and Ph.D. degrees from Kyoto University, Kyoto, Japan in 1988 and 2000, respectively. He joined NTT radio communications systems labs., Yokosuka, Japan, in 1988. In 1997, he was seconded to ATR adaptive communications research laboratories, Kyoto, Japan. From 2000 to 2002, he worked for NTT DoCoMo, Yokosuka, Japan. In 2002, he moved to DoCoMo communications laboratories Europe GmbH, Germany. From 2004 to 2011, he worked as an associate professor at Kyoto University. Since 2011, he is a full professor at graduate school of natural science and technology, Okayama University. From the beginning of his research carrier, he has been engaged in the research and development of digital mobile radio communications. In particular, he has considerable interests in channel equalization, array signal processing, Space time codes, spatial multiplexing, and multimode reception. He received the Excellent Paper Award and the communication society best paper award from IEICE in 1995 and 2020, respectively.

Yafei Hou received the B.S. degree in electronic engineering from the Anhui University of Technology and Science, China, in 1999, the M.S. degree in computer science from Wuhan University, China, in 2002, and the Ph.D. degrees from Fudan University, China, and the Kochi University of Technology, Japan, in 2007. He was a Post-Doctoral Research Fellow with Ryukoku University, Japan, from 2007 to 2010. He was a Research Scientist with Wave Engineering Laboratories, ATR Institute International, Japan, from 2010 to 2014. From 2014 to 2016, he was an Assistant Professor with the Graduate School of Information Science, Nara Institute of Science and Technology, Japan. Since 2017, He has been an assistant professor at gradulate school of natural science and technology, Okayama University, Japan. His research interests are communication systems, wireless networks, and signal processing. He is a senior member of IEEE and senior member of IEICE.